Documentation of Changes Supported by Close-range Surface-based Photogrammetry

Shahaf LEVIN and Sagi FILIN, Israel

Key words: Change detection, surface-matching, close-range photogrammetry, surface-based photogrammetry

SUMMARY

The need to monitor and document changes in observed scenes is an important application in many disciplines. Changes can appear in different scales, ranging from obvious changes, such as entire object being removed from or introduced to the scene, to barely noticeable ones such as object deformations. Image-based change detection methods utilize intensity data and image-processing techniques coupled with 3D point clouds based methods to detect changes in object-space, usually either by computing point-to-point differences or performing segmentation and classification of the data and detecting changes in objects. Nevertheless, these methods are only suitable for dense data and collapse when sparse data is used. Several photogrammetric methods have also been proposed for documentation of changes in various forms, but the stochastic nature of the observation is almost always ignored there.

We present in this paper a surface based block-alignment model and its consequent application for change documentation from close-range images. Change-detection is based on outlier analysis method associated with geodetic network design and measurement. We discuss the application of proposed model for the documentation project of an archeological excavation site. Results show that the model applies well to close-range photogrammetry and can also be used for feature extraction.

Documentation of Changes Supported by Close-range Surface-based Photogrammetry

Shahaf LEVIN and Sagi FILIN, Israel

1. INTRODUCTION

The need to monitor and document changes in observed scenes is an important application in many disciplines. Changes can be in different scales, ranging from obvious changes, such as entire object being removed from or introduced to the scene, to barely noticeable changes such as object deformations.

Reviewing the body of research that has been devoted for this topic shows its application in various fields. Image-based change detection methods utilize image intensity data and image processing techniques to detect changes. Intensity variation between images can be attributed to a number of factors such as illumination changes, camera movement and changes within the scene. Radke and Roysam (2005) review modern images based change detection algorithms that are applied as preprocessing steps in to filter "unimportant" changes while maintaining "significant" ones relating to actual changes in the scene. The authors present several illumination-invariant algorithms and statistical hypothesis test. However, in presence of changes in camera position, perspective changes prevent making image-based methods suitable.

Change detection based on 3D point clouds is also an active field of research. Vu et al. (2004) propose an automatic method for airborne LiDAR-based change detection. A computation of differences between "pre" and "post" grids, based on LiDAR data is implemented, and potential changes are detected according to their distance from the mean value in a difference histogram. Vogtle and Steinle (2004) propose change detection methodology in urban area following disastrous events. Instead of computing simple DSM difference they use region growing and segmentation procedure to detect buildings, and then compare building parameters. Lindenbergh and Pfeifer (2005) present another segmentation based method using terrestrial laser scanner, after the segmentation test statistics are used to detect changes. These methods make use of dense 3D point clouds associated with LiDAR and do not apply to photogrammetric data which are sparse by nature.

Ladstaedter and Kaufman (2004) present a change detection of a mountain slope based on terrestrial photogrammetry. The authors subtract DTMs extracted form images acquired from a fixed position at multiple epochs. Habib et al. (2001) present a surface-matching based change detection method based on a point-to-surface registration of two datasets which is suitable for use with sparse data. Points which do not correspond to the surface after the registration are declared as changes. Both methods ignore the stochastic nature of photogrammetric observations and process.

The application of terrestrial photogrammetry for site documentation, measurement and reconstruction is widely known. This is due to the ease of data collection, availability of

imaging devices, ability to avoid coming into physical contact with the mapped objects, and the existence of well established photogrammetric methodologies for the documentation. Therefore, photogrammetry can be considered optimal for change-detection, where multiple campaigns are needed. When datasets are collected at different epochs, point-to-point correspondence between them cannot be assumed (and usually does not exist). Therefore point-based photogrammetry is not suitable for change-detection purpose. Surface-based photogrammetry, first introduced by Ebner and Strunz (1988), does not assume point-to-point correspondence and is suitable for use in change detection. Ebner and Ohlhof (1994), Jaw (2000) and Schenk (2000) also presented variations for surface-based photogrammetry.

We present in this paper a surface based block-alignment model and its consequent application for change documentation from closer-range images. The change-detection is based on outlier detection method associated with geodetic network design and measurement. We discuss the application of proposed model for the documentation project of an archeological excavation site. Results show that the model performs well for change-detection based on close-range photogrammetry, and can also be used for feature extraction.

2. SURFACE-BASED CHANGE DETECTION MODEL

The objective of the proposed model is to develop a method for detecting changes between two photogrammetric derived data points depicting the same site, based on image data that was acquired in different epochs. In addition, it has to account for the sparse data and resolution differences associated with photogrammetry in general and close-range photogrammetry in particular. Since change-detection requires both datasets to be in the same reference-frame the model is also required to handle registration of the datasets.

The model is based on surface-based photogrammetric registration solution utilizing outlier detection methods to identify changes between epochs. Outlier detection is first discussed, flowed by presentation of the registration model and the proposed change-detection scheme.

2.1 Outlier detection

Geodetic networks use outlier detection methods in order to screen gross errors and as means of deformation analysis. Outliers are defined as observations which do not agree with a model. There are several methods for detection of outliers associated with least-squares estimation. The common ones used in geodetic-networks are Baarda's Data-snooping (Baarda, 1968), Tau-test and Danish method (Berberan, 1992).

Data-snooping is rooted in probability theory and utilizes hypothesis tests. The null hypothesis is that no outliers exist, and the alternative hypothesis is that only one gross error exists. However, in practice this method allows for detection of multiple outliers in an iterative manner. It is based on the assumption that the a priori standard deviation (*std.*) of a unit-weight observation σ_0 is known, and is used to calculate the standard deviation of the residuals. Normalized residuals u_i are then calculated and used as

$$u_i = \frac{|v_i|}{\sigma_0 \sqrt{q_{v_i v_i}}} \tag{1}$$

with v_i the residual of the ith observation and q_{vivi} the element in the cofactor matrix of the observation corresponding to that observation. u_i is used as the test value for the hypothesis test, with $u_{\alpha 0}$ the critical value (usually taken from nomograms). If the test value exceeds the critical value the corresponding observation is considered an outlier and is discarded from the dataset. Only a single outlier can be detected at a time.

The Tau-test method is similar to data snooping, but does not assume that σ_0 is known. The a posteriori *std.* $\hat{\sigma}_0$ is used to calculate the normalized residuals and to be used as test value T_i

$$u_i^{\tau} = \frac{|v_i|}{\hat{\sigma}_{v_i}} = \frac{|v_i|}{\hat{\sigma}_0 \sqrt{q_{v_i v_i}}} \tag{2}$$

Since v_i and $\hat{\sigma}_0$ are statistically dependent the *t*-distribution does not apply and u_i^{τ} is governed by the τ-distribution. τ-distribution tables are not easily accessible; however, the critical value can be calculated based of *t*-distribution values

$$\tau_f = \frac{t_{f-1}\sqrt{f}}{\sqrt{f - 1 + t_{f-1}^2}} \tag{3}$$

with *t* the *t*-distribution value and *f* the degrees of freedom. Similar to Baarda's test, if the test value exceeds the critical value the corresponding observation is considered as an outlier and is discarded from the dataset. Only a single outlier can be detected at a time.

Both data-snooping and the tau-test assume that only one outlier exists, and their underlying theoretical foundations do not apply if there is more than one outlier. While practically multiple outliers can be iteratively detected, one at a time, these methods are unsuitable for detection of multiple outliers as in the case of change-detection.

Robust estimation methods for outlier detection are purely heuristic, making no assumption about the stochastic nature of the observations. These methods are founded on the idea that large residuals indicate less accurate observations and vice-versa. Therefore, after performing the least-squares estimation, the a priori weights of the observation are replaced with functions of the residuals and the model is estimated again. This process is carried iteratively until convergence of the weights. Several reweighting function exist. The one applied by the Danish method is

$$p_{\nu+1} = \begin{cases} p_\nu & u_i^D \le c \\ p_\nu \cdot \exp\left(-\frac{u_i^D}{c}\right) & else \end{cases} \quad ; \quad u_i^D = \frac{|v_i|}{\hat{\sigma}_0}\sqrt{p_1} \tag{4}$$

with $\nu = 1,2,\ldots$ the iteration number, p_ν the weight on the ν^{th} iteration, u_i^D the normalized residual (p_1 is the weight of the observation at the first iteration), and c a critical value which is usually in the range of 2-3. After the model converges all residuals with a value greater than a given threshold are considered outliers. At this time two options are available. The first option is deleting outlying observations from the dataset and the model solving the model without them. The second is using the final estimation of the Danish method, since the final weights of the outliers should be close to zero and so they would not affect the quality of the solution.

Huber (1981) proposes a different reweigthing function

$$p_{\nu+1} = \begin{cases} p_\nu & u_i^A \le c \\ p_\nu \cdot \frac{1}{u_i^A - (c-1)} & else \end{cases} \quad ; \quad u_i^A = \frac{|v_i|}{\hat{\sigma}_0}\sqrt{p_1} \tag{5}$$

It should be noted that for the underlying assumption for the robust estimation methods to hold true, i.e., large residuals indicate less accurate observations; an estimation model with high-internal reliability should be used. Such models are characterized by high redundancy numbers, meaning that most of the observations error is absorbed in its respective residual.

2.2 Surface-based photogrammetry registration model

Surface-based photogrammetry cannot provide single-photo solutions (contrary to point and line based methods), and require at least two images. This suggests that photogrammetric-based registration of the datasets has to have some notion of 3D to 3D relation. Such relation translates into the registration of 3D datasets, which in photogrammetry relates to an absolute orientation problem. The need to determine 3D coordinates necessitates the extraction of homologous point from the images. Reliable change-detection requires a dense photogrammetric dataset, and surface-based registration greatly benefit from such dense datasets, therefore an autonomous methods for the extraction of homologous points are desirable.

2.2.1 Homologous point extraction

Several algorithms exist for extraction of homologous points in an image set, cross-correlation and least-squares matching to name a few (Schenk, 2000). These methods work well for generation of rapid 3D dataset when no substantial change exists within the imageset, such as can be found in aerial photogrammetry setups and stereo-pairs. However, when

substantial perspective changes exist between the images, such as can be found in close-range photogrammetry, these methods fail to produce reliable datasets. The Scale-Invariant-Feature-Transform (SIFT) (Lowe, 2004) method is designed to be invariant to scale, rotation, and illumination, and for practical use is invariant to sufficient amount perspective changes. The methodology consists of: i) detection of candidate interest points via scale-space extrema search, ii) localization of the keypoints, iii) orientation assignment based on the image local gradient to ensure scale and orientation invariance, and iv) descriptor computation. For each detected keypoint a descriptor which is invariant to scale, rotation and changes in illumination, is generated. The descriptor is based on orientation histograms in the appropriate scale. Each descriptor consists of 128 values.

The extraction of candidate counterpart points is vital in the present case for two purposes: the first is the establishment of the relative orientation between image pairs, and the second is launching the point-to-surface registration model. These two goals have two different objectives, the first is obtaining a reliable set of points for orientation where the focus is on their quality, and the second is obtaining a detailed surface model, with focus on quality but also on their quantity. In this regards, the ability to control the amount of keypoints extracted by the SIFT model provides an excellent and efficient means for the provision of large set of potential 3D points. Therefore, the counterpart extraction process is applied here in two parts.

For the relative orientation, a high filtering threshold is set, so that only a marginal number of outliers result. Considering the fact that for the computation of the relative orientation only five points are required, setting a high threshold still provides a great number of degrees of freedom than what is customary to use.

The computed relative orientation also defines the geometrical locus where all candidate counterparts of a given point can be found. Therefore, for second phase that concerns describing the surface, the initial filtering threshold value for potential corresponding points is decreased. Matches are not only evaluated by their descriptor similarity, but also by their proximity to the epipolar line in the second image. Proximity is computed by the image distance between a point and the epipolar line it is expected to lie on. Points whose distances exceed a certain threshold value are discarded. The distance is a function of the accuracy of the estimation of the relative orientation. Notice that outlying matches that lie along epipolar lines cannot be detected and will be identified as changes in by the change-detection scheme.

2.2.2 Surface-based registration model

With the extraction of 3D pointsets a registration model is presented. The goal of the registration is align the datasets from different epochs while enabling easy identification of outlying observations. Registration of 3D datasets requires relating entities between both datasets. Besl and McKay (1992) propose computing a rigid-body transformation in an iterative fashion by updating correspondence. Convergence is reached when the actual matches are found. Chen and Medioni (1992) proposed a point-to-surface registration scheme for determining the rigid body transformation. Parameters are based on minimizing the sum of square-distances between a pointset and a surface. Grün and Akca (2005) add a scale factor to

the algorithm. In order to accommodate the needs of close-range photogrammetry surface-based registration (i.e. occlusions and varying scale and resolution) a point-to-surface model, one epoch's data are represented as a pointset, and the other epoch's data as a surface-model. This representation assumes no correspondence between the datasets and therefore suitable for change-detection. The alignment of the datasets is done by determining the similarity transformation between the coordinate systems of both epochs. Similarity transformation is defined

$$\mathbf{p} = m \cdot \mathbf{R} \cdot (\mathbf{p}' - \mathbf{t}) \tag{6}$$

with **p'** a point in the first (*point*) epoch coordinate system, **p** a point in the second (*surface*) epoch coordinate system, **t** the translation between the two systems, **R** the orthonormal rotation matrix, and *m* the scale factor.

The common surface models are usually provided either in the form of a regular-grid or by a set of irregularly distributed points. For the latter case the triangular-irregular-network (TIN) is usually established as a surface representation. Regular grids are easy to generate, manipulate, and access, however they are limited to 2.5D and by nature limited to work with regular data. The TIN representation is more general than the regular grid model, more flexible, and can be employed to a full 3D model as well. The common use of TIN representation and its greater flexibility motivate the formulation of the solution with this representation.

The local surface patches in the TIN, defined by the three triangle vertices, are considered planar. The point-to-plane distance δ_i can then be written in vector form is

$$\delta_i = \begin{bmatrix} \mathbf{n}_i^T & d_i \end{bmatrix} \cdot \begin{bmatrix} \mathbf{p}_i \\ 1 \end{bmatrix} \tag{7}$$

with $\mathbf{n}_i = [n_i^x, n_i^y, n_i^z,]^T$ the normalized (unit length) normal vector to the plane defined by triangle t_i, d_i the plane constant, and $\mathbf{p}_i = [x_i, y_i, z_i]$. Linking Eq. (6) and Eq. (7) leads to

$$-m\mathbf{n}_i^T\mathbf{R}\mathbf{t} + m\mathbf{n}_i^T\mathbf{R}\mathbf{p}_i' + d_i - \delta_i = 0 \tag{8}$$

The origin of both coordinate systems – the *point* and the *surface* ones, are transformed to their respective centroids. The quantities in Eq. (8) can be categorized as belonging into unknowns and observations. $\mathbf{s} = [t_x, t_y, t_z, m, \omega, \phi, \kappa]^T$ is the vector of unknown transformation parameters, **p'** is the observation for the *point* epoch **n** and *d* are the observations for the *surface* epoch, and δ is the observation for the difference between the two epochs. A strong dependency exists between **p'** and [**n**, *d*] through δ. Modeling this dependency is not practical, and since the interest of the registration model is to estimate the differences between the datasets (δ) **p**', **n**, and *d* are considered as constants. Eq. (8) is non-linear, so in order to perform a least-squares estimation, linearization using Taylor series expansion leads to

$$\mathbf{As} + \mathbf{Bv}_\delta + \mathbf{w} = 0 \tag{9}$$

with **s** the differential correction to the initial transformation parameters approximations, and $\mathbf{v}_\delta$ the residuals of the distance observations, and

$$\mathbf{A} = \frac{\partial f(\mathbf{S}, \mathbf{p}, T)}{\partial \mathbf{S}} \;;\; \mathbf{B}_p = \frac{\partial f(\mathbf{S}, \mathbf{p}, T)}{\partial \delta} = -\mathbf{I}$$

The least-squares target function becomes then

$$\mathbf{s}^T\mathbf{P}_s\mathbf{s} + \mathbf{v}_\delta^T\mathbf{P}_\delta\mathbf{v}_\delta - 2\mathbf{k}^T\left(\mathbf{As} - \mathbf{v}_\delta + \mathbf{w}\right) = \min \tag{10}$$

with $\mathbf{P}_\delta$ the weight matrix for the observations, $\mathbf{P}_s$ the weight matrix for the initial values of the unknowns, and **k** the vector of Lagrange multipliers. Unless prior knowledge about the relation between the two datasets exists $\mathbf{P}_s$ usually set to zero. Solving Eq. (10) leads to

$$\hat{\mathbf{s}} = -\mathbf{N}^{-1}\mathbf{A}^T\mathbf{P}_\delta\mathbf{w} \tag{11}$$

$$\hat{\mathbf{v}}_\delta = \mathbf{A}\hat{\mathbf{s}} + \mathbf{w} \tag{12}$$

with $\mathbf{N} = \mathbf{A}^T\mathbf{P}_\delta\mathbf{A} + \mathbf{P}_s$. The a posteriori variance is given by

$$\hat{\sigma}_0^2 = \frac{\hat{\mathbf{s}}\mathbf{P}_s\hat{\mathbf{s}}^T + \hat{\mathbf{v}}_\delta\mathbf{P}_\delta\hat{\mathbf{v}}_\delta^T}{n-u} \tag{13}$$

with n the number of condition equations (equals to the number photogrammetric model points), and u the number of transformation parameters (seven here).

The initial assumption of the registration procedure is that there are no changes between epochs so that all observations are inliers. This is assumption is parallel to the null hypothesis is hypothesis tests. Since both datasets represent the same object the value of δ is set to zero. Setting the values in the weight matrices will be discussed in section 2.3.

The model was extensively tested in various simulated and real world setups and showed that redundancy numbers in the presented model are in the range of 0.7-0.9. These are exceptionally high, and well suited for detection of outliers as mentioned in section 2.1.

The discrete, piecewise, representation of the surface by the TIN model requires establishing correspondence between the points and the triangles. The model defines that a point is related to a triangle if: i) the point is inside the triangle – a vector from the point to the triangle, with direction parallel to the normal to the triangle plane, intersect the triangle plane inside of it,

and ii) the distance between the point and the triangle plane is the minimum with respect to all triangles that answer condition (i).

2.3 Change-detection scheme

Aiming for a method that can handle within the entire dataset, simultaneously, data-snooping and the tau-test that seek only one outlier within a dataset are discarded and the robust estimation method is applied. The procedure follows the next scheme:

1. Setting initial weights in $\mathbf{P}_\delta^0$.
2. Solving the registration model with the current $\mathbf{P}_\delta^\nu$ (with ν the iteration number).
3. Calculating new weights according to Eq.(4) and setting $\mathbf{P}_\delta^{\nu+1}$. c is set at the range of 1.5-3, depending on the quality of the data.
4. If $\mathbf{P}_\delta^{\nu+1}$ differ from $\mathbf{P}_\delta^{\nu+1}$ go to stage 2.
5. Declare all observation with residual higher than a threshold value as changes.

The initial values in $\mathbf{P}_\delta^0$ are set according to the expected accuracy of the 3D points reconstructed from the photogrammetric models and generally should be close to unity. Areas in the datasets (both epochs) with questionable accuracy or reliability should yield lower weights, which should be taken in account in the final stage of the procedure. It is noted that for the change-detection itself estimation of the registration parameters $\hat{\mathbf{s}}$ is not necessary and so Eqs.(11) and (12) can be combined to

$$\mathbf{v}_\delta = \left(-\mathbf{A}\mathbf{N}^{-1}\mathbf{A}^T\mathbf{P}_\delta + \mathbf{I}\right)\mathbf{w} \tag{14}$$

In the final step, when declaring changes, one should take in account observation with initial low weights. These will inherently have large residuals regardless. If these initial weights are below a threshold value (the weight corresponding to the residual size ($p_{critical} = \hat{\sigma}_0^2 / v_{critical}^2$) for declaring changes, these observation should be flagged as suspicious and might indicate gross errors during their 3D reconstruction phase.

3. RESULTS AND DISCUSSION

The application of the proposed model is demonstrated on a documentation project in Raqefet cave, an archeological excavation site in the Carmel mountain ridge, as part of an ongoing research studying the origins and use of Manmade-bedrock-holes in those sites. An excavation campaign performed on August 2008 serves as the case study for this paper. The study is performed at a small area of ~10 m^2. Images were acquired during the excavation with a Nikon D70 camera, with 48 mm Nikkor lens.

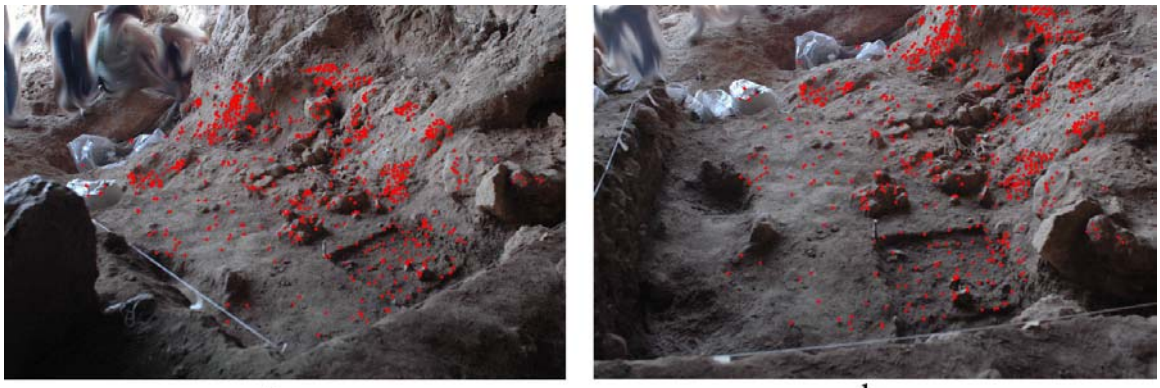

a b

Figure 1. The image-pair for the first epoch. (a) is the left image and (b) is the right image. Homologous points extracted using the SIFT algorithm are marked by red points.

For the *point* epoch two images were acquired with base length of ~1.5 m and convergence angle of ~25°. Applying the SIFT algorithm on the image set resulted in a set of 913 points that were autonomously extracted. Among them 101 points have passed the high threshold filtering stage (threshold was set to 4) and the rest where found corresponding by limiting the search to the epipolar line locus. Of the 101 points that were used for the relative orientation phase none were outliers. Similar results were observed in other stereo-pairs on which the keypoint extraction model was applied. The set of homologous points are presented in Figure 1, while being marked on the images. The extraction accuracy was ~1.5 pixels and the 3D reconstruction accuracy was 0.5 cm. The dataset of this epoch is represented as a pointset. After several artifacts were removed the site was mapped again for the *surface* epoch, which data is represented as a TIN surface-model. Both datasets were independently geo-referenced for future inspection.

At this point, with datasets corresponding to two epochs the registration and change-detection scheme is performed. Although both datasets are geo-referenced, and therefore their relative pose and orientation can be computed, the seven similarity transformation parameters are treated as unknowns and their weight matrix $\mathbf{P}_s$ is set to zero. The initial weight matrix for the observation $\mathbf{P}_\delta^0$ is set as an identity matrix. Danish method is used of reweighting and the critical value is set to $c = 2$ and. The weight critical value for declaring a change is set to $p_{\text{critical}} = 0.1$, which correspond to a critical residual value of $3\sigma_0$. The objects that were removed from the site between the epochs are shown highlighted in Figure 2a. while Figure 2b. shows the results of the change-detection procedure on one of the images. Changes that were detected are indicated by green points, changes that are no detected by yellow points and red points indicate points that were falsely detected as changes. Sixty seven points were manually identified as part of a removed object and thus should be identified as changes. Sixty four of those points (96%) were successfully identified and only three were not. All the unidentified points were sampled close to ground and therefore are not considered as change. Six points which were not part of a removed object was identified as changes.

a b

Figure 2. The changes between epochs were manually detected and highlighted in (a). (b) shows the results of the change-detection procedure. Green points indicated successful change detection, yellow indicate changes which were not detected, and red indicate false detections.

Error! Reference source not found.a. shows the behaviour of the weight matrix $\mathbf{P}_\delta$ throughout the iterations. The mean weights for observations inside and outside of the change area, indicated by solid red and blue lines respectively, clearly show convergence of the detection procedure at the sixth iteration. The dashed black line indicates the critical weight $P_{\text{critical}} = 0.1$. Setting higher values for the critical value c in the re-weighting step (c=2 here) will yield faster convergence, but may lead to more false detections. The dashed blue line indicates the minimal weights for observation in non-changing areas of the site. At the point of convergence the red and dashed-blue lines are practically cannot be separated. This is do to the rapid convergence of the exponent function used for weighting used by Danish method.

3.1 Use for object extraction

It is noted that the same procedure used for change-detection can be used, with slight modification, for feature extraction. In the change-detection model the datasets are defined temporally according to their acquisition epoch. Applying the same model on a coarse surface-model of site terrain and an unclassified pointset, containing both terrain and objects, will result in detecting points outlying with respect to the surface-model, thus classify them as objects or new details.

4. CONCLUSIONS

This paper has demonstrated the utilization of surface-based photogrammetry as a basis for a robust-estimation change detection model. It has shown how combining the two allow for fast and reliable change-detection in close-range scenes, detecting almost all the changes while making only a marginal number of false detections. The use of registration model for change-detection relieves the need for establishing control network, and the use of a surface based model relives the need of identifying corresponding points in the image set. Such models are useful for the documentation changes in various sites with no need to access the site.

REFERENCES

Baarda, W., 1968, A Testing Procedure for Use in Geodetic Networks. *Publ. Geod. New Ser.*, **2**, 27-55.

Berberan, A., 1992. Outlier Detection and Heterogeneous Observations a Simulation Case study. *Aust. J.Geod. Photogramm. Surv.*, **56**, 49-61.

Besl, P. and McKay, N. 1992. A Method for Registration of 3-D Shapes. *Trans. on PAMI*, **14**(2), 239 - 256.

Chen, Y., Medioni, G., 1992.Object modeling by registration of multiple range images. *Image and Vision Computing* **10**(3), 145–155.

Ebner H. and Strunz, G., 1988. Combined Point Determination Using Digital Terrain Models as Control Information. *Int. Archives of Photogrammetry and Remote Sensing*, **27**(B11), III/578-587.

Ebner H. and Ohlhof T, 1994. Utilization of Ground Control Points for Image Orientation without Point Identification in Image Space. *Int. Archives of Photogrammetry and Remote Sensing*, **30**(3/1), pp. 206-211.

Grün A. and D. Akca, 2005. Least squares 3D surface and curve matching. *ISPRS Journal of Photogrammetry &Remote Sensing* **59**(3), 151–174.

Habib, A., Lee, Y., Morgan, M., 2001. Surface Matching and Change Detection Using the Modified Hough Transform for Robust Parameter Estimation. *Photogrammetric Record*, **17**(98), pp. 303-315.

Huber, P.J., 1981, In *Robust Statistics*. Wiley: New York.

Jaw, J.J., 2000. Control Surface in Aerial Triangulation. *International Archives of Photogrammetry and Remote Sensing*. **33**(3B).

Ladstaedter, R., Kaufmann, V., 2005. Change Detection of A Mountain Slope by Means of Ground-Based Photogrammetry: A Case Study in The Austrian Alps. *4th ICA Mountain Cartography Workshop.*

Lindenbergh, R., Pfeifer, N., 2005. A Statistical Deformation Analysis of Two Epochs of Terrestrial Laser Data of A Lock. *In Proceedings of the 7th Conference on Optical 3- D measurement techniques*, Vienna, Austria. pp. 61-70

Lowe, D.G. 2004. Distinctive Image Features from Scale-Invariant Keypoints. *International Journal of Computer Vision*. **60**(2), pp. 91-110.

Radke, R., Roysam, B., 2005. Image Change Detection Algorithms: A Systematic Survey. *IEEE Transactions on image processing*. 14(3).

Schenk ,T., 2000. Digital Photogrammetry, Volume I: Background, Fundamentals, Automatic Orientation Procedures. Terra Science.

Vögtle, T., Steinle, E., 2004. Detection and Recognition of Changes In Building Geometry Derived From Multitemporal Laserscanning Data. *In Proceedings of the XXth ISPRS Congress*. July 12-23, 2004 Istanbul, Turkey. pp. 428-433.

Vu, T., Matsuoka, M., Yamazaki, F., 2004. LIDAR-Based Change Detection of Buildings in Dense Urban Areas. *IEEE International Geoscience and Remote Sensing Symposium (IGARSS '04)*.

CONTACTS

Mr. Shahaf Levin
Transportation and Geo-Information Eng
Technion – Israel Institute of Technology
Borowitz Building, Technion City
Haifa, 32000
ISRAEL
Tel. +972-4-8292482
Fax + 972-4-8295708
Email: shahafl@technion.ac.il

Dr. Sagi Filin
Transportation and Geo-Information Eng
Technion – Israel Institute of Technology
Rabin Building, Technion City
Haifa, 32000
ISRAEL
Tel. +972-4-8295855
Fax + 972-4-8295708
Email: filin@technion.ac.il